Lifetime Benchmarking of Two DC-link Passive Filtering Configurations in Adjustable Speed Drives

Haoran Wang[1], *Student Member, IEEE*, Pooya Davari[1], *Member, IEEE*, Huai Wang[1], *Senior Member, IEEE*, Dinesh Kumar[2], *Member, IEEE*, Firuz Zare[3], *Senior Member, IEEE*, and Frede Blaabjerg[1], *Fellow, IEEE*

1. Department of Energy Technology, Aalborg University, Denmark
2. Global Research & Development Center, Danfoss Drives A/S, Denmark
3. School of Information Technology and Electrical Engineering Faculty of Engineering, The University of Queensland, Australia

hao@et.aau.dk; pda@et.aau.dk; hwa@et.aau.dk; dinesh@danfoss.com; f.zare@uq.edu.au; fbl@et.aau.dk

***Abstract*—Electrolytic capacitors with a DC-side inductor, and the slim DC-link capacitor are two typical filtering configurations in Adjustable Speed Drives (ASDs). The reliability performance of these capacitive DC-link solutions is an essential aspect to be considered, which depends on both component inherent capability and the operational conditions (e.g., electro-thermal stresses) in the field operation. This paper studies the reliability performance of the LC filter and slim capacitor based filter in a standard ASD system. Considering the variations of the capacitor parameters, environment stresses, and lifetime model, the lifetime of the two configurations are compared. Moreover, scalability analysis is presented in terms of power rating, amplitude and phase angle unbalance levels at the grid side. The results serve as a guideline for reliability aspect performance benchmarking of different DC-link solutions in ASD applications.**

I. Introduction

Adjustable Speed Drive (ASD) systems have been widely used as an effective energy saving solution in various industrial, commercial and residential applications [1], [2]. DC links are an important part of a standard ASD, in terms of size, cost, and reliability. It serves to limit the DC-link voltage ripple, absorb harmonics, and provide a certain amount of energy storage for abnormal and transient operations [3], [4]. In many power electronic applications, the DC-link LC filter requires relatively high energy storage, and electrolytic capacitors are widely used due to its cost-effectiveness and energy density. However, the use of electrolytic capacitor raises reliability concern. The primary cause of electrolytic capacitor degradation is due to electrolyte evaporation and electro-chemical reaction, which highly depend on the electro-thermal stresses. High ripple currents cause internal self-heating, increasing the hot-spot temperature, and resulting in aging. Moreover, it can cause the increase of capacitor Equivalent Series Resistor (ESR) over time. Because an increase in its ESR causes more heating for a given ripple current, thus increasing the core temperature rise and accelerating the degradation process. Thus, for capacitor sizing in DC-link LC filter, the reliability performance is an essential aspect to be investigated. It depends on both the inherent capability of the selected capacitors and the operational conditions (e.g., electro-thermal stresses) in the field operation [5], [6]. In recent years, small DC-link capacitors utilizing film capacitor have been paid more attention by power electronics and drive manufactures, due to reduced line current harmonics emission and potential to improve reliability [7]. However, a comprehensive analysis of the lifetime estimation and comparison between the conventional LC filters and slim capacitor DC-link solutions do not exist in the literature.

Modern distribution networks still face different power quality issues such as voltage unbalance, background harmonic distortion, voltage sag, swell and line frequency variation, etc. Recent power quality issues show that among the different types of power quality disturbances, unbalanced voltage has the most frequent occurrence in many distribution networks [8, 9]. During voltage unbalance events, three-phase diode rectifiers may enter in single-phase operation mode (depending on the load level and unbalance level), which can generate low-order harmonic components (100 Hz, 200 Hz at 50 Hz mains) in the DC-link voltage. These low-order voltage harmonics result in undesirable impact on electro-thermal stresses, and therefore, the reliability of the DC-link capacitors. The DC-link capacitor stress under one specific operating condition is studied in [10], and the reliability of the DC-link capacitor under different operating conditions is worth to being studied.

From the reliability point of view, there are the following limitations in prior studies: 1) No quantitative lifetime comparison between the two filters is available. 2) The grid unbalance situation could alter the electro-thermal stresses of key components in a motor drive [11–13]. The impact of the grid voltage amplitude and phase angle unbalance on the lifetime of the two cases is not described. 3) lack of Physical-of-Failure (PoF) understanding for lifetime prediction [14].

The purpose of this paper is to benchmark the reliability of the two DC-link configurations in drives under different grid conditions. Although [10] discussed the electrical stress of capacitor in drives, however the reliability analysis and benchmarking between the two DC-link configurations under different grid conditions is not provided. This paper develops a mission profile based lifetime estimation procedure for capacitors considering the nonlinear accumulated damage and accelerated degradation process. Based on the proposed lifetime

978-1-5386-1180-7/18/$31.00 ©2018 IEEE

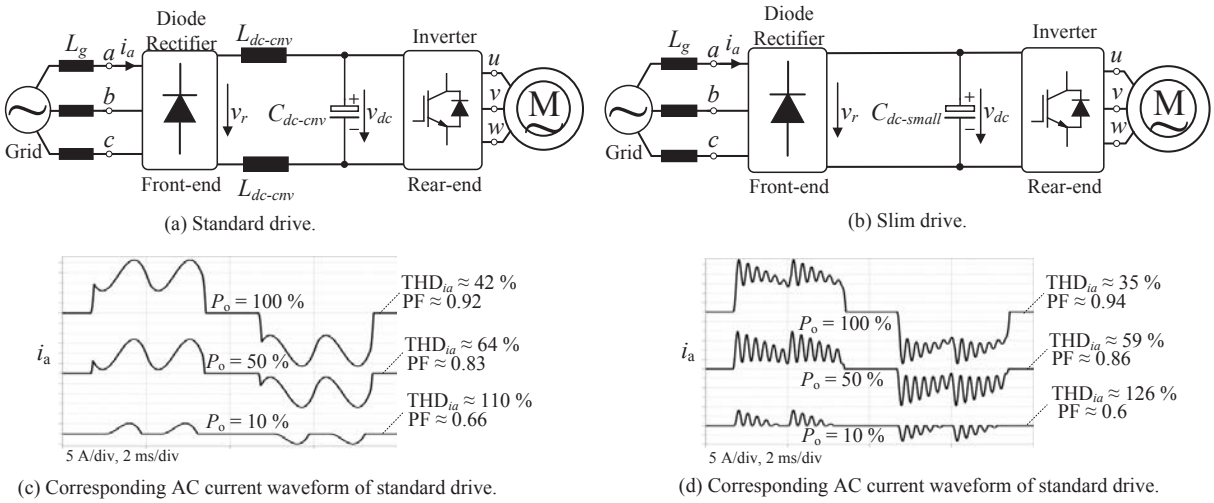

Fig. 1. A block diagram of the ASD system with two kinds of DC-link configurations and corresponding AC current waveforms under balanced operation at different loads.

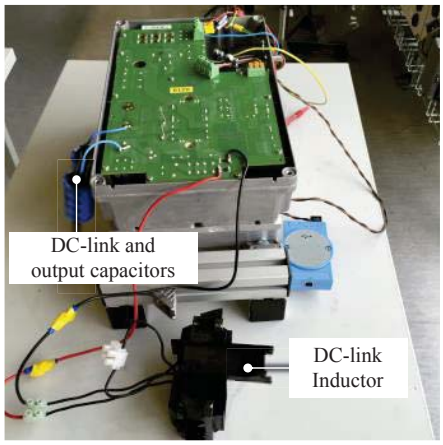

Fig. 2. Experimental prototype of the motor drive.

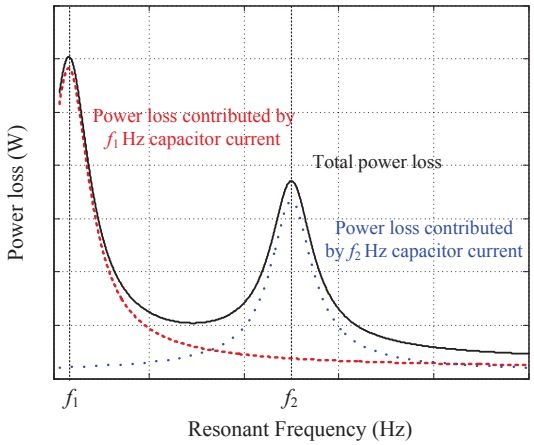

Fig. 3. Schematic diagram to show the relation between resonant frequency and the power loss of capacitor.

estimation procedure, the reliability performance benchmarking between the DC-link LC filter and the slim capacitor in ASDs under balanced and unbalanced grid voltage conditions is investigated.

The rest of this paper is organized as follows. In section II, the system structure with two DC-link configurations are described. In section III, the lifetime estimation procedure is presented. Experimental case studies under different operational conditions are presented in section IV, followed by the conclusion.

II. Description of the Study Case

Fig. 1 shows a block diagram of the three-phase motor drives investigated in this paper, and the corresponding AC current waveforms. The experimental prototype is shown in Fig. 2. Fig. 1 (a) shows the first case which is implemented with a DC-link LC filter. The conventional drive has a large size DC or AC inductor in order to reduce the line current harmonics as well as a large DC capacitor to limit the DC-link voltage fluctuation. Fig. 1 (b) presents the second case, where the ASD utilizes a small DC-link capacitor. One of the main problems is the resonant frequency generated by the DC-link capacitor and the line inductance (L_g). The line inductance of a low-voltage distribution network is mainly defined by the size and the type of the step-down transformer.

Ripple current stress is an important stressor that affects the DC-link capacitor lifetime. According to the circuit analysis, the capacitor current spectrum can be divided into two frequency ranges: 0-2 kHz (i.e., Low-frequency harmonics introduced by unbalanced input and output power) and above 2 kHz (i.e., high-frequency harmonics introduced by the power electronic switching). The Root Mean Square (RMS) current at the specific frequency depends on the following factors: 1) The operating status of the ASDs, and the grid conditions: such as during voltage unbalance events, three-phase diode rectifier may enter in single-phase operation mode, which generates low-order harmonic components in DC-link voltage. These

low-frequency harmonics alternate the electrical loadings of the DC-link capacitors. Therefore, the reliability performance estimated under balanced grid operation conditions is no longer valid. 2) Different DC-link configurations have different impedance characteristics, in terms of resonant frequency, damping coefficient, and so on, resulting in different gain at the frequency of interest. The schematic diagram in Fig. 3 is to show the relationship between the resonant frequency and the power loss of the DC-link capacitor. f_1 Hz and f_2 Hz harmonics in the capacitor current are considered for illustrations. The power loss contributed by f_1 Hz current reaches the peak when the resonant frequency is f_1 Hz. With a higher resonant frequency, the gain at f_1 Hz decreases, so that the power loss decreases. Similar phenomenon can be obtained from the power loss contributed by f_2 Hz capacitor current. The power loss reaches the peak value when the resonant frequency is f_2 Hz. Thus, from the total power loss, it can be seen that the resonant frequency has impact on the power loss of the capacitor, which affects the lifetime of the capacitor.

III. Reliability Evaluation of Capacitors

The proposed reliability evaluation procedure for capacitors is shown in Fig. 4. The procedure includes three major steps: electrical-thermal loading analysis, nonlinear damage accumulation, and Monte-Carlo simulation based variation analysis. A mission profile (i.e., ambient temperature, load condition) is applied as the input. The output is the lifetime of the capacitor with a certain confidence level (e.g., 90 %). The feedback loop from the accumulated damage to the electrical model of the capacitor shows the accelerated degradation effect, corresponding to the capacitance reduction and the ESR increase. The purpose of the method is to provide a systematic lifetime estimation procedure to evaluate the capacitor reliability, which is based on lifetime models and specified mission profile. Following the procedure, lifetime benchmarking of capacitors under different application or loading conditions can be provided. A detailed discussion on the procedure is provided in the following.

A. Electro-thermal Loading Analysis

Thermal stress is a critical stressors to capacitor wear out. The ripple current and ambient temperature are the contributors to the capacitor hot-spot temperature. For electrolytic capacitors, the dominant degradation mechanisms are electrochemical reaction in the oxide layer and the electrolyte vaporization [3]. Both factors lead to an increase of ESR over time. Especially, the increase of capacitor power loss causes a higher operating temperature inside the capacitor. The hot-spot temperature of the capacitor, which is effected by the current stress and ambient temperature, is presented by

$$T_{\mathrm{h}} = T_{\mathrm{a}} + R_{\mathrm{ha}} \times \sum_{i=1}^{n} [ESR(f_{\mathrm{i}}) \times I_{\mathrm{rms}}^2(f_{\mathrm{i}})] \qquad (1)$$

where T_{h} is the hot-spot temperature, T_{a} is the ambient temperature, R_{ha} is the equivalent thermal resistance from hot-spot to ambient, $ESR(f_{\mathrm{i}})$ is the equivalent series resistance at frequency f_{i}, $I_{\mathrm{rms}}(f_{\mathrm{i}})$ is the RMS value of the ripple current at frequency f_{i}.

B. Accumulated Damage Considering Wear Out and Random Failure

1) Nonlinear Accumulated Damage Model: For electrolytic capacitors and film capacitors, a widely used lifetime model is as [3]:

$$L = L_0 \times (\frac{V}{V_0})^{-p_1} \times 2^{\frac{T_0 - T_{\mathrm{h}}}{p_2}} \qquad (2)$$

where L_0, V_0, V, T_0 and T_{h} are the rated lifetime, rated voltage, real voltage, ambient temperature and hot-spot temperature of the capacitor. For film capacitor, the exponent p_1 is from around 7 to 9.4, which is used by leading capacitor manufacturers. For electrolytic capacitors, the value of p_1 typically varies from 3 to 5. p_2 is a coefficient around 10. From above equation, it can be seen that the lifetime is a function of T_{h} which is the hot-spot temperature of the capacitor.

The nonlinear accumulated damage model is developed to describe the real damage progress. The wear out of the capacitor represents as increase of ESR. The formulated model that accounts for the effects of these processes, but without a specific identification is represented by

$$a = a_0 + (a_{\mathrm{f}} - a_0) r^{\mathrm{q}} \qquad (3)$$

where a_0, a, and a_{f} are normalized ESR growth at initial, instantaneous, and final state, respectively; q is a function of lifetime N and material constants, and r is the ratio $n_{\mathrm{i}}/N_{\mathrm{i}}$, where n_{i} and N_{i} are the instantaneous equivalent operating time and total lifetime under the same loading condition, respectively. Damage is then defined as the ratio of instantaneous to final ESR growth. In most cases, $a_0 = 0$, and the damage function becomes

$$D = r^{\mathrm{q}} \qquad (4)$$

The extended nonlinear accumulated model is

$$D_{\mathrm{n}} = \left[\left(\frac{n_{\mathrm{i}-1}}{N_{\mathrm{i}-1}} \right)^{\frac{q_{\mathrm{i}-1}}{q_i}} + \frac{n_{\mathrm{i}}}{N_{\mathrm{i}}} \right]^{q_{\mathrm{i}}} \qquad (5)$$

2) Equivalent Hot-spot Temperature Derivation: By accumulating the damage, the dynamical stresses are converted into static values for each type of temperature stress. Taking the accumulated damage to the lifetime model, the equivalent hot-spot temperature can be derived inversely.

$$T_{\mathrm{h,eq}} = -p_2 \ln \left[D_{\mathrm{n}} \times \frac{1}{L_0} \times \left(\frac{V}{V_0} \right)^{-p_1} \right] + T_0 \qquad (6)$$

C. Monte-carlo Analysis and Lifetime Prediction

The application of the lifetime model results in a fixed accumulated damage. It is far from reality since the capacitor parameter variations and the statistical properties of the lifetime model are not considered. In field operations, the time to end-of-life for the capacitor could vary within a range due to the tolerance in physical parameters and the difference in the experienced stresses. Therefore, a statistical approach based on Monte-Carlo simulations is applied. Especially, the distributions of the temperature-related lifetime constants L_0, p_2 and the temperature tolerance-related parameter T_{h} are plotted. Different values of constants result into different

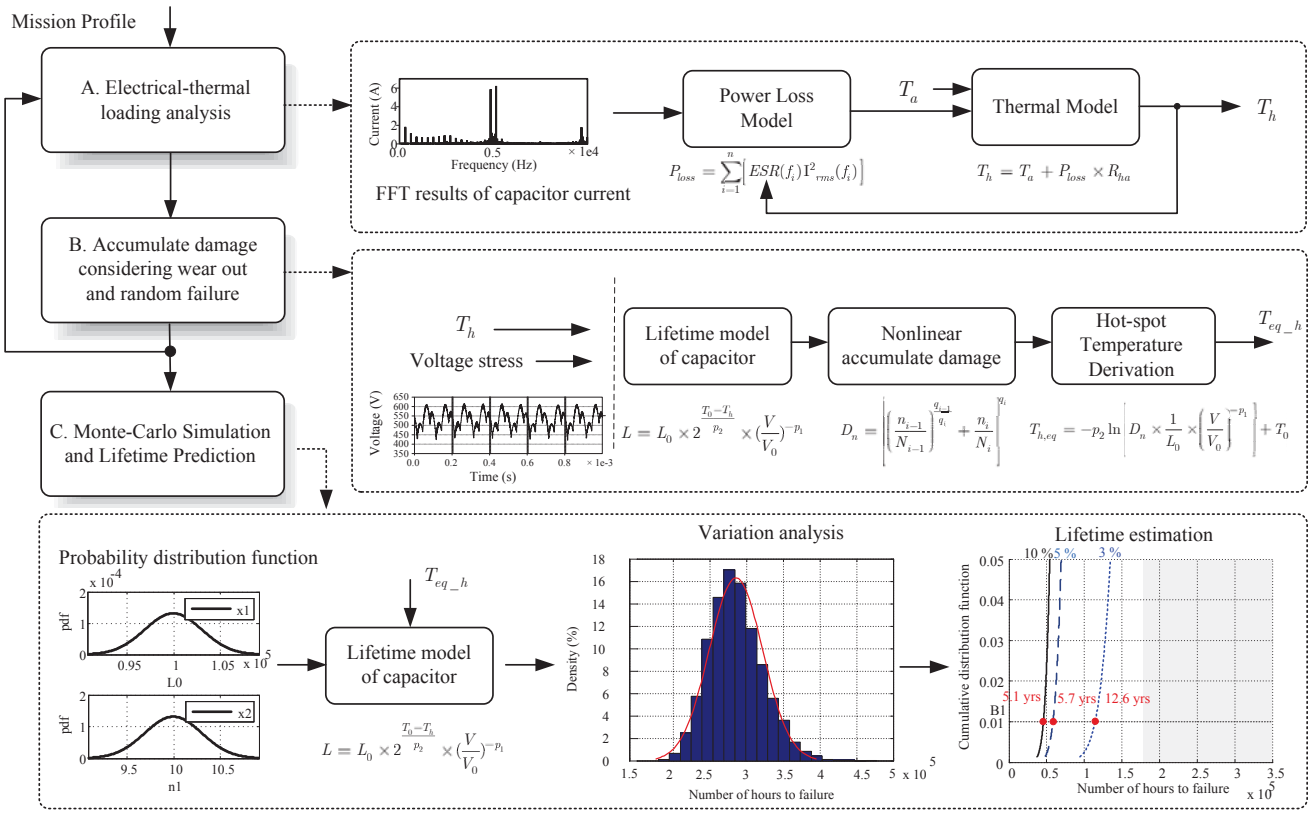

Fig. 4. Lifetime estimation procedure of the capacitors in the two different ASD system.

TABLE I
SPECIFICATION OF THE MOTOR DRIVE AND THE DC-LINK CONFIGURATIONS.

Motor drive specifications		Standard LC filter based drive		Slim capacitor configuration
Rated power (kW)	7.5	Physical configurations	Four 450V/680uF electrolytic capacitors	1000 V/ 30 uF Film capacitor
Grid phase voltage (V)	230	ESR of single capacitor	150 mΩ @100 Hz	20 mΩ @100 Hz
Switching frequency (kHz)	5	Thermal resistance	5.3 ℃/W	12 ℃/W
DC-link voltage (V) @ 7.5 kW balanced grid voltage	535	Rated load lifetime	5000 hours @105℃ and rated ripple current	100000 hours @70℃ and rated ripple current
Ambient temperature (℃)	45	$L_{DC\text{-}cnv}$	1.25 mH	

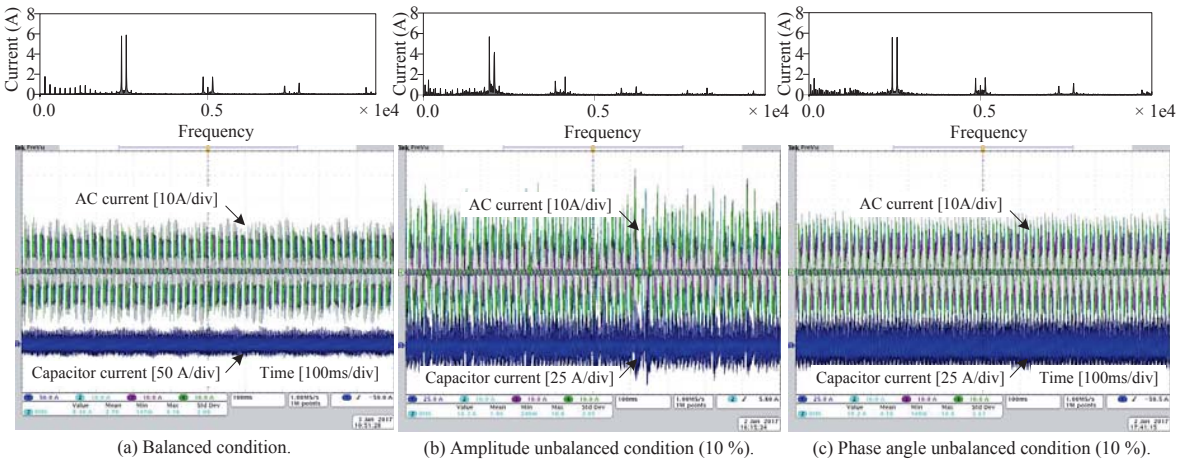

(a) Balanced condition. (b) Amplitude unbalanced condition (10 %). (c) Phase angle unbalanced condition (10 %).

Fig. 5. Experimental results of ASD system with a slim capacitor operating at 5kW.

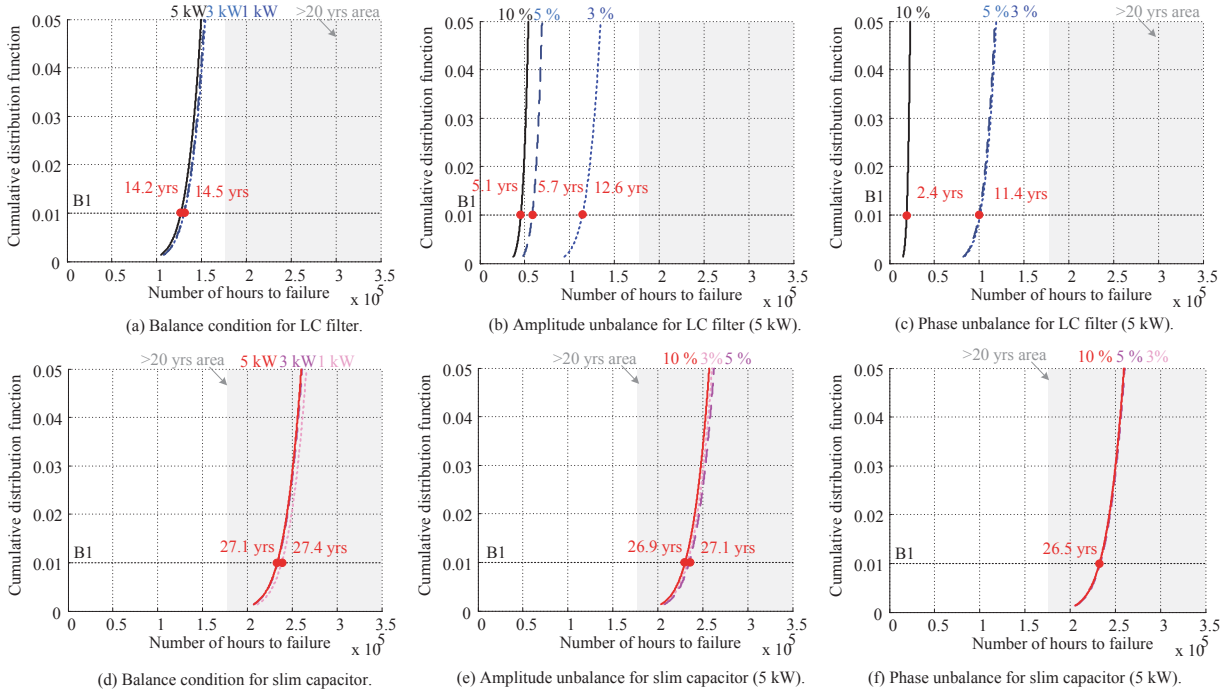

(a) Balance condition for LC filter.
(b) Amplitude unbalance for LC filter (5 kW).
(c) Phase unbalance for LC filter (5 kW).
(d) Balance condition for slim capacitor.
(e) Amplitude unbalance for slim capacitor (5 kW).
(f) Phase unbalance for slim capacitor (5 kW).

Fig. 6. Lifetime estimation results of the ASD system with two DC-link configurations.

lifetimes. Then, the sensitivity of the lifetime to L_0, p_2 and T_{h} can be evaluated individually or collectively. Finally, the distribution of the end-of-life of the capacitors can be obtained, allowing a lifetime analysis with a specified confidence level.

D. Feedback for Electrical Analysis Due to Capacitance Reduction

Along with the damage accumulated, the capacitance reduction and ESR growth result in a increasing DC-link voltage ripple and changing the current spectrum of the DC-link current, which accelerates the degradation process of the electrolytic capacitor. A feedback loop is considered in the lifetime estimation procedure to represent the accelerated degradation.

IV. Scalability Analysis

An experimental prototype is shown in Fig. 2, and the specification of the experimental setup is shown in Table I. In this study, the lifetime analysis for the two DC-link configurations is conducted, in terms of power rating, amplitude, and phase angle unbalanced conditions. Experimental results of ASD system with a slim capacitor operating at 5kW are shown in Fig. 5 to illustrate the impact.

Following the lifetime estimation procedure, the lifetime of the two DC-link configurations are shown in Fig. 6. Under balanced condition, with the increasing output power of the system, the lifetime of the two cases decrease. Compared with the conventional LC filter, the slim capacitor has longer lifetime under balanced condition. With the increasing of the grid unbalance, the reliability becomes different. For the LC filter, the lifetime is significantly reduced, such as the scenarios of 5 % and 10 % amplitude unbalance, and 10 % phase unbalance. The reason is that the low-frequency harmonics introduced by the unbalanced condition are increasing with the unbalance level and further amplified by the resonant oscillation, where the resonant frequency of the LC filter is around 120 Hz. For the slim capacitor, under amplitude unbalance condition, the lifetime does not decrease with the increasing unbalance level. The high frequency harmonics around the resonant frequency play a more critical role compared with the low frequency harmonics, while it has insignificant impact on the thermal loading.

V. Conclusion

This paper studies the reliability performance of the two DC-link passive filtering configurations. The capacitor lifetime for the two cases have been studied under different operating conditions. It can be concluded that: 1) For the presented case study, the lifetime of the LC filter DC-link configuration is relatively shorter than that of the slim capacitor, especially under amplitude and phase unbalanced conditions. 2) It quantifies that significant impact of the power rating and grid conditions for the two configurations, which should be considered in the concept-phase and design-phase of a motor drive development.

References

[1] F. Zare, H. Soltani, D. Kumar, P. Davari, H. A. M. Delpino, and F. Blaabjerg, "Harmonic emissions of three-phase diode rectifiers in distribution networks," *IEEE Access*, vol. 5, pp. 2819–2833, 2017.

[2] M. Hinkkanen and J. Luomi, "Induction motor drives equipped with diode rectifier and small dc-link capacitance," *IEEE Trans. Ind. Electron.*, vol. 55, no. 1, pp. 312–320, Jan. 2008.
[3] H. Wang and F. Blaabjerg, "Reliability of capacitors for dc-link applications in power electronic converters-an overview," *IEEE Trans. Ind. Appl.*, vol. 50, no. 5, pp. 3569–3578, Sep. 2014.
[4] H. Wen, W. Xiao, X. Wen, and P. Armstrong, "Analysis and evaluation of dc-link capacitors for high-power-density electric vehicle drive systems," *IEEE Trans. Vehicular Tech.*, vol. 61, no. 7, pp. 2950–2964, Sep. 2012.
[5] B. Sun, X. Fan, C. Qian, and G. Zhang, "Pof-simulation-assisted reliability prediction for electrolytic capacitor in led drivers," *IEEE Trans. Ind. Electron.*, vol. 63, no. 11, pp. 6726–6735, Nov. 2016.
[6] VISHAY, General Technical Information.
[7] M. Hinkkanen and J. Luomi, "Induction motor drives equipped with diode rectifier and small dc-link capacitance," *IEEE Trans. Ind. Electron.*, vol. 55, no. 1, pp. 312–320, Jan. 2008.
[8] Council of European Energy Regulators (CEER), 5th Ceer Benchmarking Report on the Quality of Electricity Supply, 2011.
[9] S. Elphick, P. Ciufo, G. Drury, V. Smith, S. Perera, and V. Gosbell, "Large scale proactive power-quality monitoring: An example from australia," *IEEE Trans. Power Del.*, vol. 32, no. 2, pp. 881–889, Apr. 2017.
[10] K. Lee, T. M. Jahns, G. Venkataramanan, and W. E. Berkopec, "Dc-bus electrolytic capacitor stress in adjustable-speed drives under input voltage unbalance and sag conditions," *IEEE Trans. Ind. Appl.*, vol. 43, no. 2, pp. 495–504, Mar. 2007.
[11] D. Kumar, P. Davari, F. Zare, and F. Blaabjerg, "Analysis of three-phase rectifier systems with controlled dc-link current under unbalanced grids," in *IEEE APEC*, Mar. 2017, pp. 2179–2186.
[12] X. Pei, W. Zhou, and Y. Kang, "Analysis and calculation of dc-link current and voltage ripples for three-phase inverter with unbalanced load," *IEEE Trans. Power Electron.*, vol. 30, no. 10, pp. 5401–5412, Oct. 2015.
[13] H. Wang, P. Davari, D. Kumar, F. Zare, and F. Blaabjerg, "The impact of grid unbalances on the reliability of dc-link capacitors in a motor drive," in *Proc. IEEE ECCE*, Oct. 2017, pp. 4345–4350.
[14] D. Zhou, H. Wang, and F. Blaabjerg, "Lifetime estimation of electrolytic capacitors in a fuel cell power converter at various confidence levels," in *IEEE SPEC*, Dec. 2016, pp. 1–6.